

This article was downloaded by:

On: 21 January 2011

Access details: *Access Details: Free Access*

Publisher *Taylor & Francis*

Informa Ltd Registered in England and Wales Registered Number: 1072954 Registered office: Mortimer House, 37-41 Mortimer Street, London W1T 3JH, UK



The Journal of Adhesion

Publication details, including instructions for authors and subscription information:

<http://www.informaworld.com/smpp/title~content=t713453635>

Modelling Cyclic Moisture Uptake in an Epoxy Adhesive

A. Mubashar^a; I. A. Ashcroft^a; G. W. Critchlow^b; A. D. Crocombe^c

^a Wolfson School of Mechanical and Manufacturing Engineering, Loughborough University, Loughborough, Leicestershire, UK ^b Institute of Surface Science & Technology, IPTME, Loughborough University, Loughborough, Leicestershire, UK ^c Division of Mechanical, Medical, and Aerospace, University of Surrey, Guildford, UK

To cite this Article Mubashar, A. , Ashcroft, I. A. , Critchlow, G. W. and Crocombe, A. D.(2009) 'Modelling Cyclic Moisture Uptake in an Epoxy Adhesive', The Journal of Adhesion, 85: 10, 711 – 735

To link to this Article: DOI: 10.1080/00218460902997224

URL: <http://dx.doi.org/10.1080/00218460902997224>

PLEASE SCROLL DOWN FOR ARTICLE

Full terms and conditions of use: <http://www.informaworld.com/terms-and-conditions-of-access.pdf>

This article may be used for research, teaching and private study purposes. Any substantial or systematic reproduction, re-distribution, re-selling, loan or sub-licensing, systematic supply or distribution in any form to anyone is expressly forbidden.

The publisher does not give any warranty express or implied or make any representation that the contents will be complete or accurate or up to date. The accuracy of any instructions, formulae and drug doses should be independently verified with primary sources. The publisher shall not be liable for any loss, actions, claims, proceedings, demand or costs or damages whatsoever or howsoever caused arising directly or indirectly in connection with or arising out of the use of this material.

Modelling Cyclic Moisture Uptake in an Epoxy Adhesive

A. Mubashar¹, I. A. Ashcroft¹, G. W. Critchlow², and
A. D. Crocombe³

¹Wolfson School of Mechanical and Manufacturing Engineering,
Loughborough University, Loughborough, Leicestershire, UK

²Institute of Surface Science & Technology, IPTME, Loughborough
University, Loughborough, Leicestershire, UK

³Division of Mechanical, Medical, and Aerospace, University of Surrey,
Guildford, UK

This paper presents a methodology for predicting moisture concentration in an epoxy adhesive under cyclic moisture absorption-desorption conditions. The diffusion characteristics of the adhesive were determined by gravimetric experiments under cyclic moisture conditions and the dependence of diffusion coefficient and saturated mass uptake on moisture history was determined. Non-Fickian moisture absorption was observed during absorption cycles while moisture desorption remained Fickian. The diffusion coefficient and saturated moisture content showed variation with absorption-desorption cycling. A finite element-based methodology incorporating moisture history was developed to predict the cyclic moisture concentration. A comparison is made between the new modelling methodology and a similar method that neglects the moisture history dependence. It was seen that the concentration predictions based on non-history dependent diffusion characteristics resulted in over-prediction of the moisture concentration in cyclic conditioning of adhesive joints. The proposed method serves as the first step in the formulation of a general methodology to predict the moisture dependent degradation and failure in adhesives.

Keywords: Cyclic moisture diffusion; Epoxy adhesive; Finite element user models

1. INTRODUCTION

Adhesive joining is an attractive alternative to conventional joining methods, such as welding and mechanical fasteners, especially in the aerospace and automobile industries. The benefits of adhesive bonding

Received 21 November 2008; in final form 24 March 2009.

Address correspondence to I. A. Ashcroft, Wolfson School of Mechanical and Manufacturing Engineering, Loughborough University, Loughborough, Leicestershire LE11 3TU, UK. E-mail: i.a.ashcroft@lboro.ac.uk

include: the ability to form lightweight; high stiffness structures; joining of different types of materials; better fatigue performance; and reduction in the stress concentrations observed with mechanical fasteners or the effects on the adherend of the heat associated with welding. However, concerns about the durability of adhesive joints still hinders their widespread use in structural applications. Moisture has been identified as one of the major factors affecting joint durability. This is especially important in applications where joints are exposed to varying moisture conditions throughout their useful life. Moisture has an adverse effect on adhesive strength, which decreases with increasing moisture content [1,2]. Plasticisation and swelling of adhesives occur with moisture diffusion and are among the major factors considered responsible for the changes in strength [3].

Fickian diffusion has been used by researchers to predict moisture concentration in adhesives [4,5]. In Fickian diffusion it is assumed that the moisture flux is directly proportional to the concentration gradient in a material and, thus, the concentration of moisture at a point in a plane sheet of thickness $2l$ may be determined by

$$C_t = \left(1 - \frac{4}{\pi} \sum_{n=0}^{\infty} \frac{(-1)^n}{2n+1} e^{-\frac{D(2n+1)^2 \pi^2 t}{4l^2}} \cos \frac{(2n+1)\pi x}{2l} \right) \times C_{\infty}, \quad (1)$$

where C_t is moisture concentration at any time interval t , C_{∞} is the saturated moisture concentration, D is the diffusion coefficient, and x is the spatial coordinate. The mass uptake, M_t , at any time interval, t , obtained by integrating Eq. (1) over the domain, is given by

$$M_t = \left(1 - \frac{8}{\pi^2} \sum_{n=0}^{\infty} \frac{1}{(2n+1)^2} e^{-\frac{D(2n+1)^2 \pi^2 t}{4l^2}} \right) \times M_{\infty}. \quad (2)$$

Fickian diffusion is observed in polymers well above the glass transition temperature (T_g) [6]. At temperatures below T_g , a non-Fickian moisture uptake is observed, where the diffusion process deviates from Fickian behaviour after initial uptake. Several models have been suggested to predict non-Fickian uptake behaviour [7–10] including a dual Fickian model, which is based on two Fickian processes operating in parallel [11]. The concentration at any point may be determined by

$$C_t = \left(1 - \frac{4}{\pi} \sum_{n=0}^{\infty} \frac{(-1)^n}{2n+1} e^{-\frac{D_1(2n+1)^2 \pi^2 t}{4l^2}} \cos \frac{(2n+1)\pi x}{2l} \right) \times C_{1\infty} \\ + \left(1 - \frac{4}{\pi} \sum_{n=0}^{\infty} \frac{(-1)^n}{2n+1} e^{-\frac{D_2(2n+1)^2 \pi^2 t}{4l^2}} \cos \frac{(2n+1)\pi x}{2l} \right) \times C_{2\infty}, \quad (3)$$

where $C_{1\infty}$ and $C_{2\infty}$ are the saturated concentrations, D_1 and D_2 are the diffusion coefficients, and l is the length of the diffusion path. The mass uptake for the dual Fickian model at any time, t , is given by

$$M_t = \left(1 - \frac{8}{\pi^2} \sum_{n=0}^{\infty} \frac{1}{(2n+1)^2} e^{-\frac{D_1(2n+1)^2\pi^2 t}{4l^2}} \right) \times M_{1\infty} + \left(1 - \frac{8}{\pi^2} \sum_{n=0}^{\infty} \frac{1}{(2n+1)^2} e^{-\frac{D_2(2n+1)^2\pi^2 t}{4l^2}} \right) \times M_{2\infty}, \quad (4)$$

where $M_{1\infty}$ and $M_{2\infty}$ are the saturated masses and the sum of $M_{1\infty}$ and $M_{2\infty}$ gives the total saturated mass. The dual Fickian model is largely phenomenological and, hence, does not provide an insight into the mechanisms of anomalous uptake; however, it is a convenient method of representing anomalous behaviour for modelling purposes.

Diffusion coefficient, D , and saturated moisture content, M_{∞} , are frequently determined using a single experimental moisture uptake curve [9,12,13]. However, it has been observed that the diffusion in a polymer is dependent on hygroscopic history. Lefebvre *et al.* [14] related the diffusion coefficient in polymers to temperature, strain, and penetrant concentration while considering a non-Fickian driving force and found good correlation with experimental data [15]. Lin and Chen [16] studied the moisture diffusion characteristics of a DGEBA/DDA epoxy system by exposing it to a sorption-desorption-resorption cycle. The desorption and second absorption were faster than the original absorption, showing an increase in the diffusion coefficient. Also, the equilibrium water content of the resorption process was greater than the sorption process. This indicated that the material properties changed with moisture cycling. In service environments, where adhesives are subjected to significant changes in humidity, the hygroscopic history has to be considered in order to determine accurately the moisture concentration. This is necessary as it provides the basis for the determination of hygroscopic stresses, strength degradation, and failure and, thus, should be incorporated in predictive modelling methods. However, few attempts have been made to study the diffusion characteristics of an adhesive under cyclic environmental conditions and, hence, predictive models currently neglect moisture history effects.

The work presented in this paper characterises the diffusion behaviour of an epoxy adhesive over multiple absorption-desorption cycles. The dependence of D and M_{∞} on cyclic moisture diffusion are studied by experimentation and a model is proposed to predict diffusion over multiple cycles. In the second part of the paper, a finite element (FE) approach is used to introduce a methodology for the prediction

of moisture concentration based on cyclic moisture-dependent diffusion parameters. A comparison of the developed methodology with a similar FE method in which moisture history is neglected is presented, where both methods are used to predict the water concentration in a single lap joint exposed to cyclic humidity conditions. This work serves as a first, and necessary step, in the development of a cyclic aging strength prediction methodology.

2. CHARACTERISATION OF CYCLIC MOISTURE UPTAKE

The history-dependent moisture sorption properties of a rubber toughened epoxy adhesive were determined experimentally. The adhesive used was FM73-M (Cytac Engineered Materials Inc., Havre de Grace, MD, USA) and comes with a polyester knitted carrier for support and handling purposes.

Before preparation of the bulk samples, the adhesive was brought to room temperature, in a desiccator, from its storage temperature of -24°C . Bulk samples of 1-mm thickness were prepared by stacking multiple layers of the adhesive film, each of 0.12-mm thickness. During manufacture, the layers were compressed using a steel roller to ensure that air trapped between the layers was released as this helps to minimize the formation of voids during curing. The adhesive layup was placed in a mould and cured in a hot press at 120°C for 1 hour [17]. The bulk samples of dimensions $60 \times 40 \times 1$ mm were cut from the cured layup.

The moisture diffusion properties of the adhesive were determined by the gravimetric method using the procedures and guidelines in [18]. Before commencing the environmental conditioning, the bulk samples were dried in an oven at 50°C to constant weight. Two sets of three samples were conditioned at 50°C , immersed in deionised water. This temperature is well below the glass transition temperature of the adhesive, which has been reported to be 99.7°C when cured at 120°C for 1 hour [19]. The samples were subjected to three absorption-desorption cycles in which the desorption was carried out in a dry oven at 50°C until a constant weight was achieved. An AL204 electronic balance from Mettler-Toledo GmbH, Laboratory & Weighing Technologies, Grefensee, Switzerland, with 0.1 mg accuracy, was used to weigh the samples at predetermined time intervals during conditioning.

The percentage moisture content in the bulk adhesive, m_t , at any time, t , is given by

$$m_t = \frac{m_2 - m_1}{m_1} \times 100, \quad (5)$$

where m_1 is the mass of the specimen after initial drying and before immersion and m_2 is the mass of the specimen at a specified time, t .

3. EXPERIMENTAL RESULTS

Figure 1 shows the average percentage mass uptake as a function of \sqrt{t}/l from the absorption and desorption experiments. Repeatability of the tests was good with a standard deviation of 11%. Considering the first

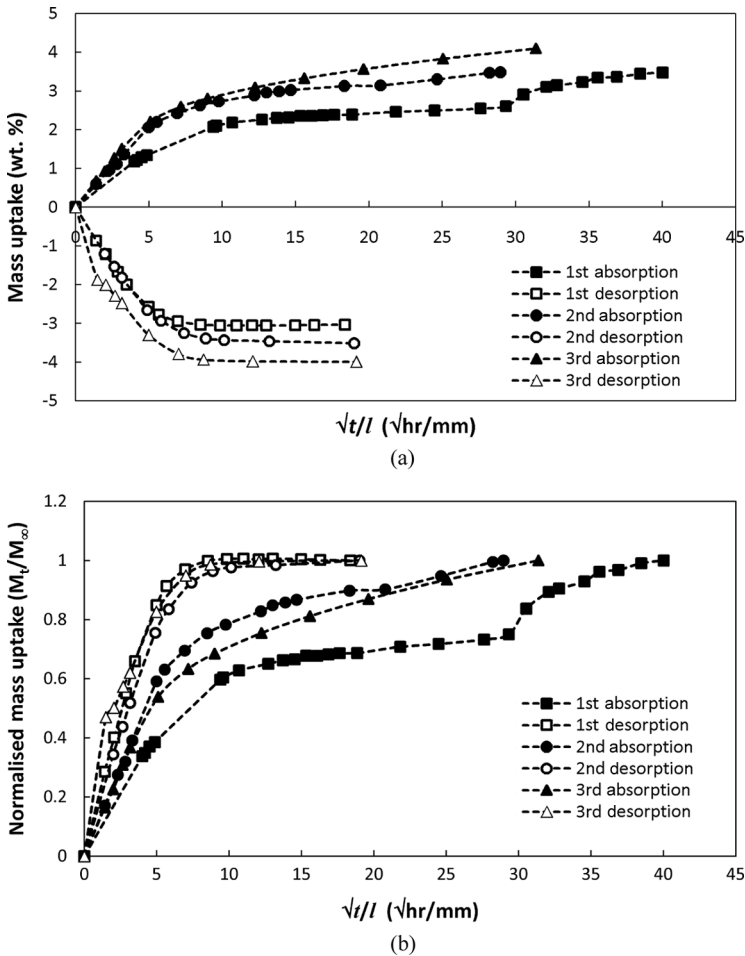


FIGURE 1 Moisture absorption and desorption curves for 1-mm thick FM73 bulk adhesive when conditioned at 50°C, immersed in water (a) mass uptake by wt.% and (b) normalised mass uptake.

moisture uptake, the rate of absorption is faster during the initial stages of diffusion. At later stages, the absorption deviates from the initial uptake trend and follows a different gradient. The overall diffusion coefficient does not remain constant and changes with increasing concentration. After reaching an apparent equilibrium, the first absorption plot shows a sudden increase in mass uptake at \sqrt{t}/l of approximately $28 \sqrt{\text{hr}/\text{mm}}$. Similar behaviour has been reported previously [20] and may be due to leaching of the adhesive during conditioning. In the later stages of diffusion, swelling, chain scission, and micro-cracking of the adhesive may occur. This can cause low molecular weight material to leach out at later stages of diffusion. These mechanisms would be irreversible and, thus, no substantial effect would be observed in further absorption cycles. The chemical composition of the polymer has a strong impact on the diffusion properties. Hygroscopic polymers, such as epoxies, have polar groups with strong affinity for water molecules and the significant interaction between the moisture and the polymer can result in a high dependence of D on concentration. It is clear from the experimental observations that a Fickian diffusion-based absorption model is inadequate in explaining the moisture uptake.

In the first desorption, diffusion takes place until a constant weight is achieved as in a Fickian diffusion process. The desorption process is clearly not the reverse of the absorption process. This is seen more clearly in Fig. 1(b) in which nominal mass uptake is used and the desorption plots are included to allow direct comparison with the absorption plots. These results indicate a physical change in the polymer structure during absorption. A constant D Fickian diffusion indicates that free water removal was the major process in desorption. It was also noted that the bulk adhesive samples achieved their original weight after desorption and the desorption process was faster than the absorption, which is a further indication of changing adhesive structure due to moisture ingress. During the absorption process, mechanisms such as chemical binding of water, swelling, and micro-cracking take place whilst in desorption the diffusion of free water is the dominant mechanism.

Full saturation was not achieved during absorptions as the samples were conditioned for a predetermined time. M_∞ and D were estimated by least square fitting of a dual Fickian model to the experimental data. The curve fitting was carried out in MathCAD using the genfit function, which employs an optimised Levenberg-Marquardt method [21]. The results of the dual Fickian curve fits are plotted in Fig. 2(a) and the coefficients of the dual Fickian model are given in Table 1. Although the dual Fickian model did not provide an exact curve fit to the first absorption due to the presence of the secondary uptake, the fit is

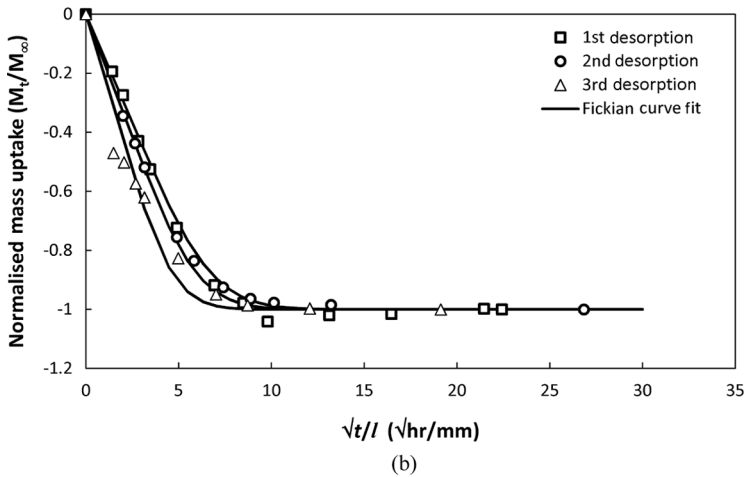
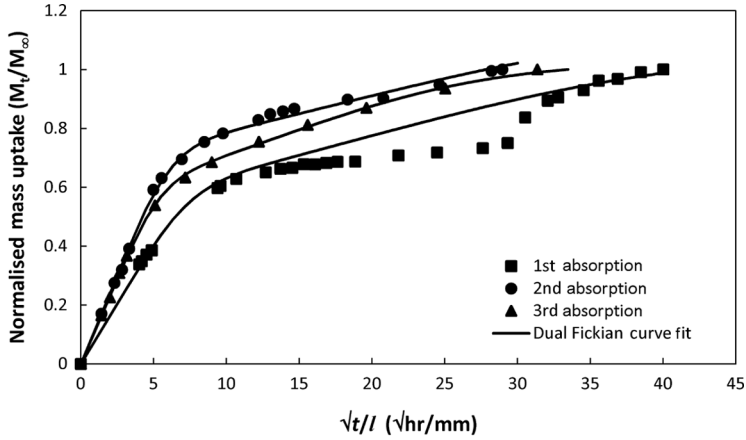


FIGURE 2 Curve fits of experimental moisture uptake for 1-mm thick samples when conditioned at 50°C, immersed in water (a) absorption and (b) desorption.

considered adequate as the model provides a reasonable prediction of the initial and final uptake and the secondary uptake requires further study. Moreover, the dual Fickian model provides an excellent fit to the resorption plots. The desorption process was modelled using Fickian diffusion and it is seen in Fig. 2(b) that this provides a good fit to the desorption plots. The coefficients of the Fickian model are given in Table 2.

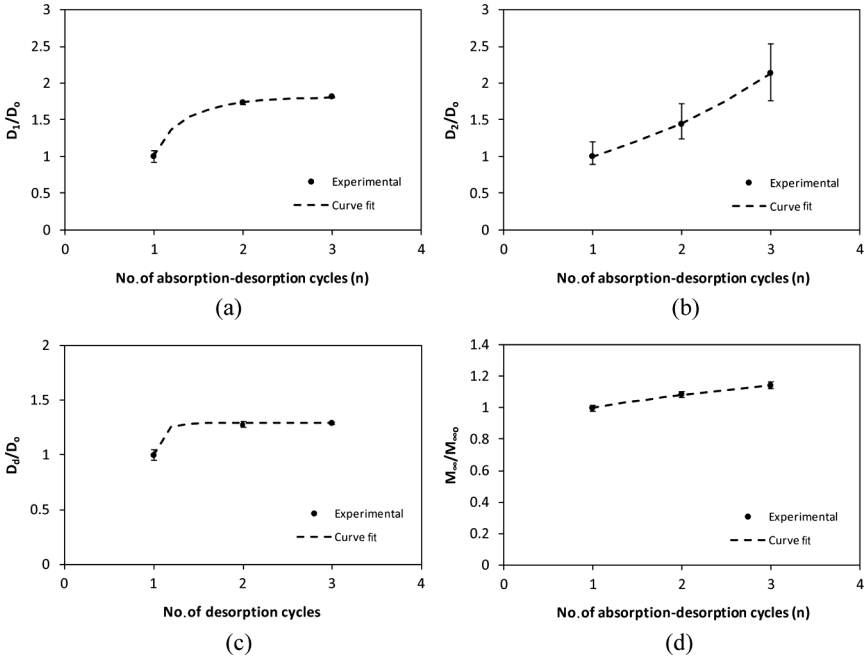
Summarising the absorption-desorption cycling, the absorption exhibits non-Fickian behaviour while desorption follow Fickian diffusion.

TABLE 1 Coefficients of Dual Fickian Model Determined by Curve Fitting to Absorption Data

Diffusion cycle	D_1 , mm ² /hr	D_2 , mm ² /hr	$M_{1\infty}$, wt. %	$M_{2\infty}$, wt. %
1st absorption	3.51×10^{-3}	1.12×10^{-4}	1.78	1.92
2nd absorption	6.04×10^{-3}	1.62×10^{-4}	2.32	1.68
3rd absorption	6.35×10^{-3}	2.39×10^{-4}	2.23	1.97

TABLE 2 Coefficients of Fickian Model Determined by Curve Fitting to Desorption Data

Diffusion cycle	D , mm ² /hr	M_{∞} , wt. %
1st desorption	4.21×10^{-3}	3.7
2nd desorption	5.39×10^{-3}	4.0
3rd desorption	5.39×10^{-3}	4.2

**FIGURE 3** Changes in moisture diffusion characteristics for FM73 over multiple absorption-desorption cycles (a) D_1 , (b) D_2 , (c) D_d , and (d) M_{∞} .

The secondary uptake behaviour observed during the first absorption was not observed in further absorption cycles. The absorption-desorption cycling caused an increase in D and M_∞ . In the dual Fickian model, D_1 increased most between the first and second absorptions while D_2 showed a more linear increase over the absorption cycles, as shown in Figs. 3(a) and (b) where D_a is the absorption or desorption coefficient during the first cycle. The desorption diffusion coefficient, D_d , which was determined based on a Fickian diffusion model, increased during the first and second cycle while no increase was observed during the second and third cycles as can be seen in Fig. 3(c); M_∞ increased slightly during moisture cycling as shown in Fig. 3(d).

The diffusion parameters along with the cyclic moisture-dependent properties were used to develop a new methodology for determining the moisture concentration under cyclic humidity conditions, which is presented in the next section.

4. PREDICTION OF CYCLIC MOISTURE DIFFUSION

4.1. Finite Element Approach

The finite element method (FEM) provides a means of predicting moisture concentration in complex geometries with variable boundary conditions and allows coupling with a mechanical analysis incorporating damage and failure predictive models [22–24]. FEM is capable of modelling transient moisture diffusion but many of the commercial software packages lack a built-in capability for modelling moisture diffusion or have limited implementations. The alternative is to use a direct analogy between conduction heat transfer and moisture diffusion. Solutions to the heat conduction equation are given in [25] and correspondence between the equations of heat transfer and diffusion is described in [26]. Diffusion is governed by Fick's first and second laws, which are given in Eqs. (6) and (7):

$$F = -D \frac{\partial C}{\partial x} \quad (6)$$

$$\frac{\partial C}{\partial t} = D \frac{\partial^2 C}{\partial x^2}, \quad (7)$$

where F is the flux, D is diffusion coefficient, C is concentration, and t is time. The corresponding heat transfer equations are given in Eqs. (8) and (9):

$$F = -k \frac{\partial T}{\partial x} \quad (8)$$

$$\frac{\partial T}{\partial t} = \left(\frac{k}{c\rho} \right) \frac{\partial^2 T}{\partial x^2}, \quad (9)$$

where T is temperature, k is thermal conductivity, ρ is density, and c is the specific heat. By comparing the above equations, diffusion may be modelled by equating D with k and C with T . The ρ and c may be taken as unity for a system with a single material.

In order to incorporate the cyclic moisture dependency in a predictive model, the empirical relationships of D and M_∞ with the number of diffusion cycles, n , were determined by least squares curve fitting. As before, the curve fitting was carried out in MathCAD and the results are shown in Fig. 3. The form of functions used for curve fitting of D_1 , D_d , and M_∞ is given in Eq. (10) and that for D_2 is given in Equation (11):

$$an^b + c \quad (10)$$

$$xe^{yn}, \quad (11)$$

where a , b , c , x , and y are constants obtained by curve fitting and given in Table 3.

The overall methodology for predicting cyclic moisture diffusion is illustrated in Fig. 4. The FE model is assigned history-dependent diffusion properties determined by experimentation. Since in-built material models are not adequate for this purpose, a user subroutine was implemented, which is described in the next section. The dual Fickian diffusion may be determined by post processing the results of two Fickian diffusion models. In the case of multiple cycles, the moisture history and state of material from one analysis is transferred to the next analysis by post processing routines and the analysis may continue for any number of cycles. The detailed implementation of the user subroutine is discussed in the next section.

TABLE 3 Constants Obtained by Curve Fitting for Empirical Diffusion Characteristic Functions

Diffusion variable	a	b	c
D_1	-0.8321	-3.056	1.832
D_d	0.2884	-11.7	1.288
M_∞	0.2144	0.4574	0.7856
	x	y	
D_2	0.677	0.3814	

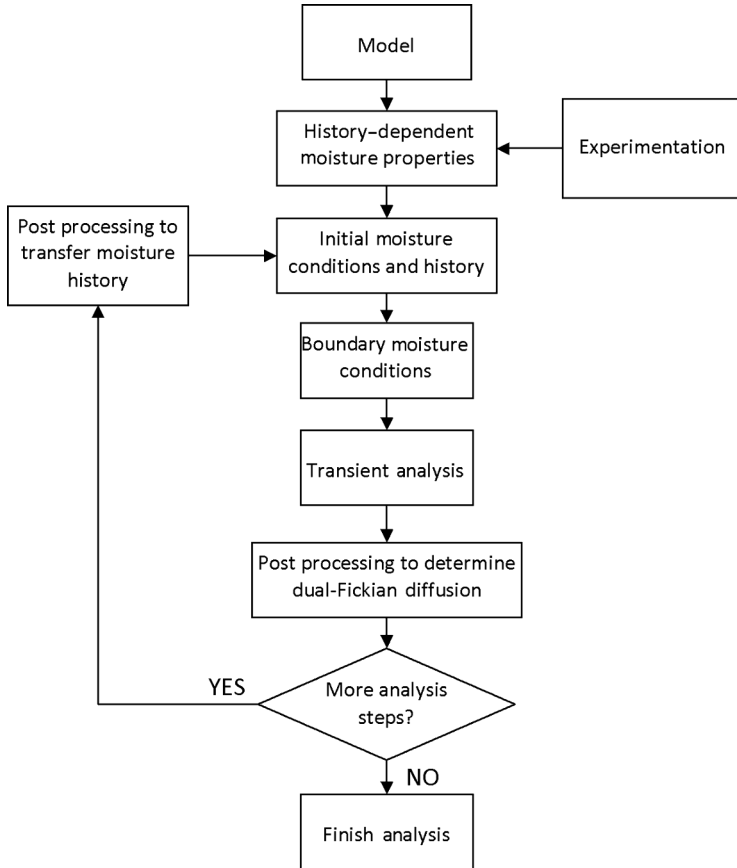


FIGURE 4 Methodology for modelling cyclic moisture diffusion.

4.2. Cyclic Moisture-Dependent Predictive Model

The cyclic moisture-dependent model was implemented in the commercial finite element code ABAQUS. Subroutine, UMATHT, is available in ABAQUS for introducing a user-defined material and was used to implement the moisture history dependence. The structure of the subroutine is illustrated by the flow chart in Fig. 5. The moisture history of the adhesive was maintained during the analysis by the use of scalar internal state variables, denoted by SV. Three state variables were used: the first state variable stores the moisture history in the form of absorption-desorption cycles; the second variable stores the nature of the diffusion

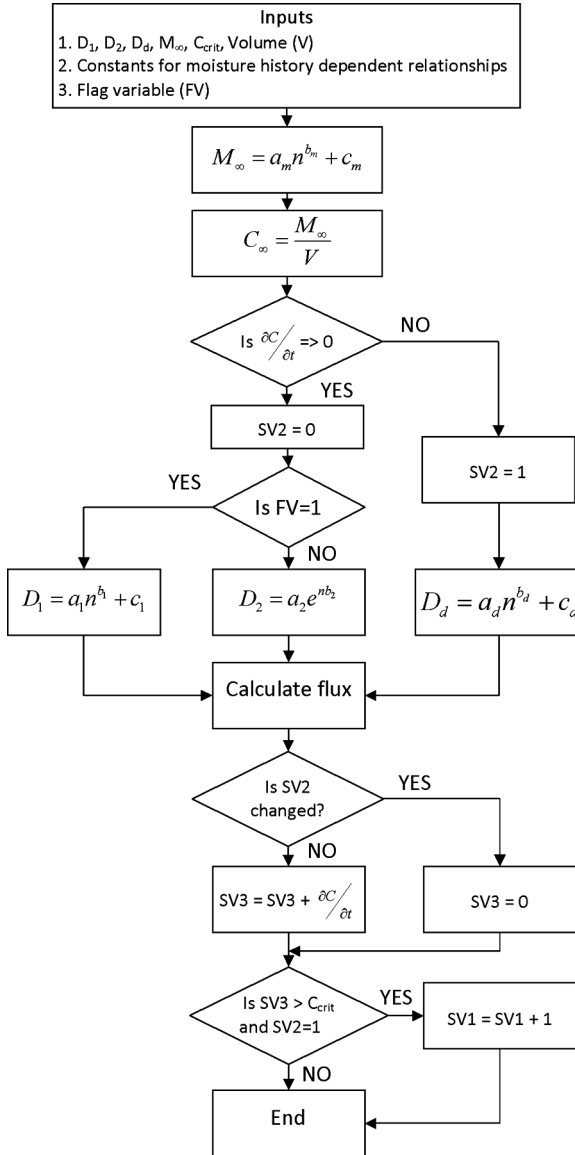


FIGURE 5 Structure of user-defined material subroutine UMATHHT.

process, *i.e.*, absorption or desorption; while the third state variable records the amount of moisture diffused during a single absorption or desorption.

The moisture cycling is based on a minimum amount of moisture absorbed in the adhesive that would change the diffusion characteristics of the adhesive. The critical concentration is an input parameter to the user subroutine, which is used to avoid minute fluctuations in moisture concentration when determining completion of a diffusion cycle. As the boundary conditions are changed, small changes in concentration may occur causing the user subroutine to determine many diffusion cycles. Thus, an absorption-desorption cycle is established when the moisture concentration at a point in the adhesive exceeds a critical concentration upon change of boundary conditions. The internal state variables were implemented as solution-dependent variables.

The history dependence of diffusion characteristics is incorporated by using the relationships developed in Section 3. The user subroutine uses a flag variable (FV) to determine the appropriate diffusion coefficients in the case of dual Fickian diffusion, where two parallel Fickian models were used to obtain the total moisture diffusion. The moisture history is transferred between sequential analyses by using a Python script and the SDVINI subroutine. SDVINI is an ABAQUS subroutine for initiating state variables.

5. COMPARISON OF MOISTURE PREDICTION METHODOLOGIES

In this section, two cases of multiple absorption-desorption in an adhesive joint are considered in order to illustrate the effect of including the cyclic moisture absorption on the prediction of moisture concentration. In the first case, the diffusion parameters are based on a single absorption curve while diffusion parameters determined from multiple absorption-desorption cycles are used in the second case, which incorporates the effects of the changes in D and M_∞ during cyclic diffusion. The history dependence of diffusion parameters is implemented *via* the developed user subroutines.

A single lap joint was modelled with aluminium adherends bonded by adhesive FM73. Diffusion was assumed to be taking place through the bulk adhesive only; *i.e.*, no interfacial diffusion was considered. However, where appropriate, interfacial diffusion can be included in the proposed modelling approach by introducing a thin layer with higher diffusion coefficient at the interface. Using symmetry, only one quarter of the adhesive layer was modelled. The adherends, as non-absorbing, did not need to be explicitly included in the model and are represented only by an insolubility boundary condition. Fillets were also not included in the model as they would not affect the

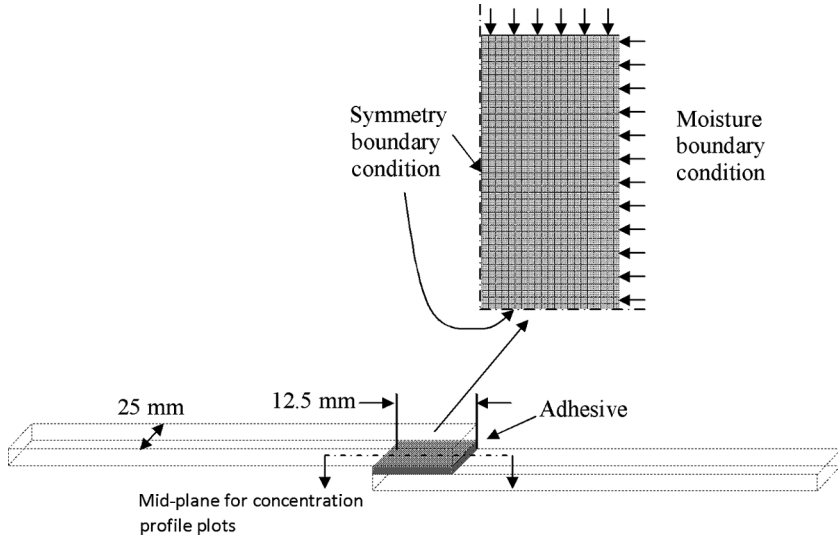


FIGURE 6 Single lap joint geometry with finite element mesh of the adhesive layer used for modelling the cyclic moisture diffusion.

comparative study. The boundary conditions were applied in the form of normalised moisture concentration and specific boundary conditions for each case are discussed later. A refined mesh with 0.3×0.3 mm, four node, linear 2D quadrilateral heat transfer field elements was used. Figure 6 illustrates the geometry of the single lap joint and the meshing of the adhesive layer.

Four cyclic conditioning environments, with absorption or desorption times of 1200, 2400, 4800, and 9600 h, were considered and each conditioning environment consisted of three absorption-desorption cycles. A typical multi-cycle conditioning environment is shown in Fig. 7, in this case with absorption and desorption cycles of 2400 h.

5.1. Case I: Predictive Modelling Using Diffusion Parameters Based on a Single Moisture Uptake Curve

The diffusion coefficients determined by curve fitting a dual Fickian diffusion model to the first experimental absorption data were used to predict concentration in the adhesive layer after multiple absorption cycles. The boundary conditions were applied in the form of normalised moisture concentration (C/C_∞). The dual Fickian model was implemented by running two sequential analyses with $D = D_1$ and $D = D_2$ and a script was used to add the concentration at each

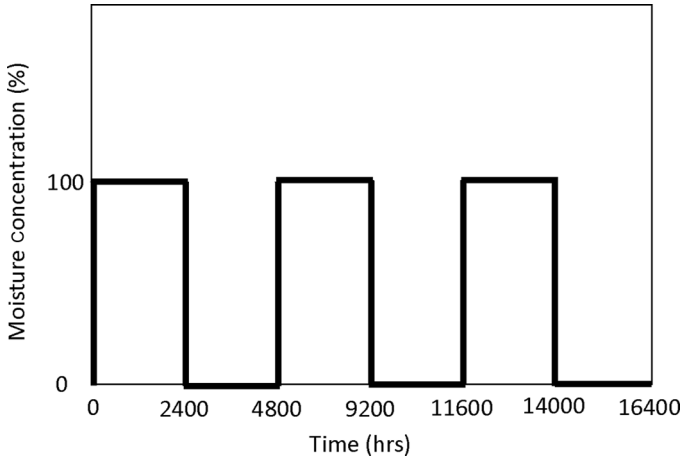


FIGURE 7 Cyclic moisture conditioning environment for finite element modelling.

integration point, providing the dual Fickian moisture uptake. The absorption cycles were followed by desorption cycles, which were based on a Fickian diffusion model. The first diffusion coefficient obtained for the dual Fickian model, D_1 , was used to predict the desorption. The concentration predicted in the first step was used as the initial concentration for the next analysis step. The analysis continued until the completion of the required environmental cycling.

Figure 8 compares concentration profiles after the first absorption for the four conditioning environments, the plots showing concentration at the centre of the adhesive layer (as illustrated in Fig. 6). It can be seen that the amount of absorbed moisture increases with absorption time; however, saturation is still not reached even after 9600 h of absorption. Figure 9 plots the moisture concentration in the adhesive layer after the first desorption cycle and shows that some moisture remains in the adhesive layer at the end of the desorption for all cycle times. The amount of moisture is a maximum at the centre of the overlap except for the desorption cycle of 1200 h. The diffusion process is governed by the moisture activity in the adhesive layer. At the start of the desorption, there is a high concentration gradient in areas close to the edges of the joint because saturation was not achieved during the previous absorption. This drives diffusion towards the centre of the overlap, in addition to the drive for diffusion towards the edges of the adhesive caused by the introduction of the “dry” boundary condition. Thus, during the initial stages of the desorption, both absorption and desorption processes are occurring simultaneously in different

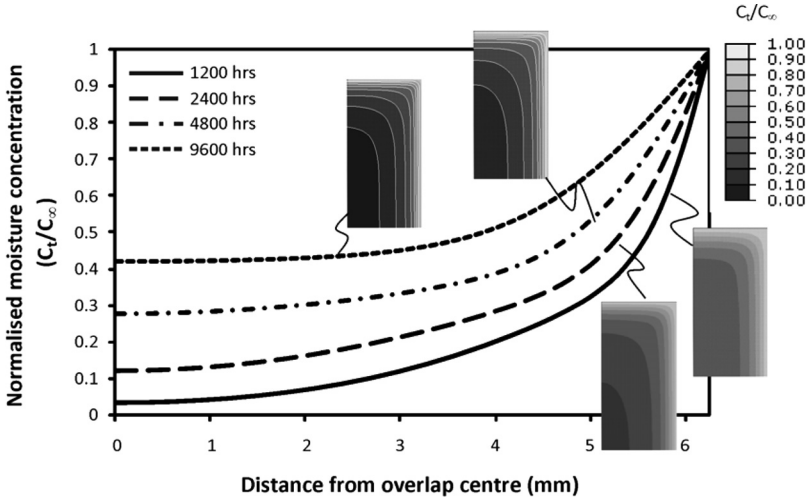


FIGURE 8 Moisture concentration in the adhesive layer after first absorption cycle.

areas of the adhesive layer. Desorption from the overlap centre starts only after a higher concentration in the surrounding material is achieved. Owing to this simultaneous absorption and desorption different parts of the adhesive may be subjected to different diffusion rates. Figure 10 shows a typical desorption process where the adhesive

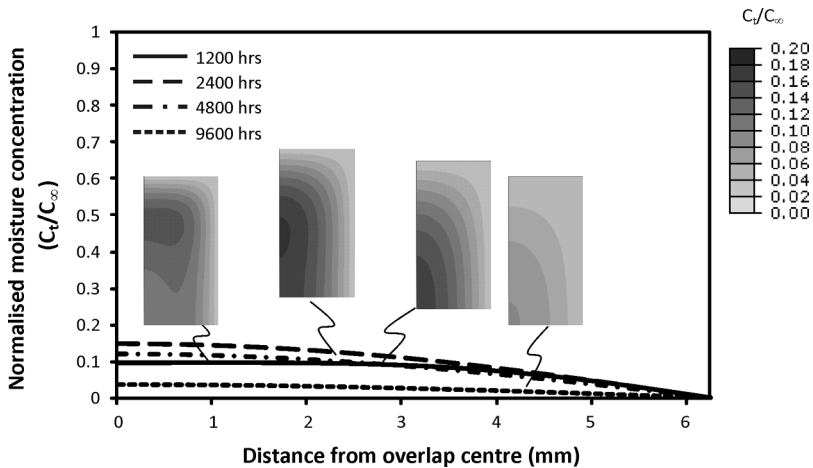


FIGURE 9 Moisture concentration in the adhesive layer after first desorption cycle.

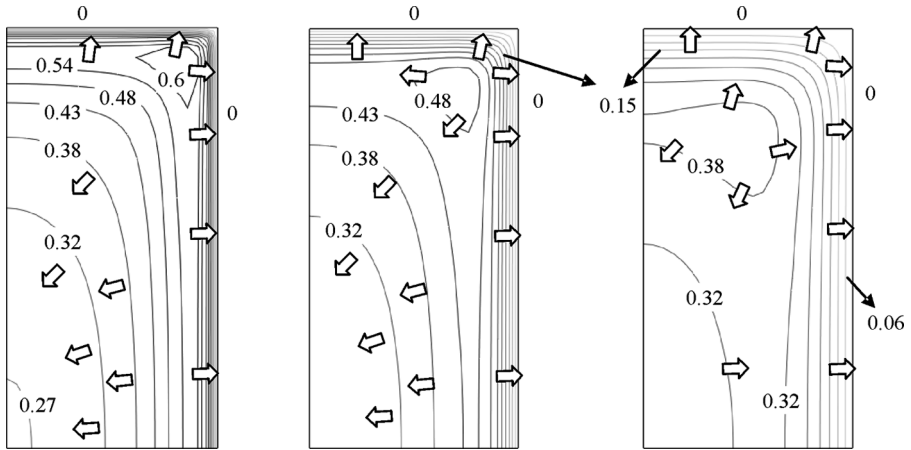


FIGURE 10 Contour plots of normalised moisture concentration in the adhesive layer during a typical desorption process. Localised concentration gradients result in simultaneous absorption and desorption in different areas of the adhesive layer. Arrows indicate direction of moisture transport.

layer is not fully saturated at the start of the desorption. As the desorption cycle starts, diffusion to the middle of the adhesive layer continues from the surrounding high concentration areas. This continues until the centre of the adhesive layer achieves a higher concentration than the surrounding material because of moisture transport towards both the edges and centre from this region.

The experimental results, as shown in Fig. 1, showed that desorption was faster than absorption and, thus, the residual moisture predicted in the adhesive layer using an absorption-based diffusion coefficient will tend to result in an over-prediction of the moisture concentration. Figure 11 compares the moisture concentration in the adhesive layer after repeated cycles of 4800 h and it can be seen that the moisture concentration increases with each absorption cycle. As the values of D and M_∞ remain constant between diffusion cycles, the increase in moisture concentration can be attributed to the residual moisture left in the adhesive after each desorption process. The amount of residual moisture also increased after each desorption as the moisture accumulated over desorption cycles; however, the increase in residual moisture becomes less with increasing number of cycles. The increase in residual moisture can be attributed to the fact that the adhesive layer did not achieve saturation during absorption and moisture flowed towards the centre of the adhesive layer from surrounding areas during subsequent cycles. The residual moisture in

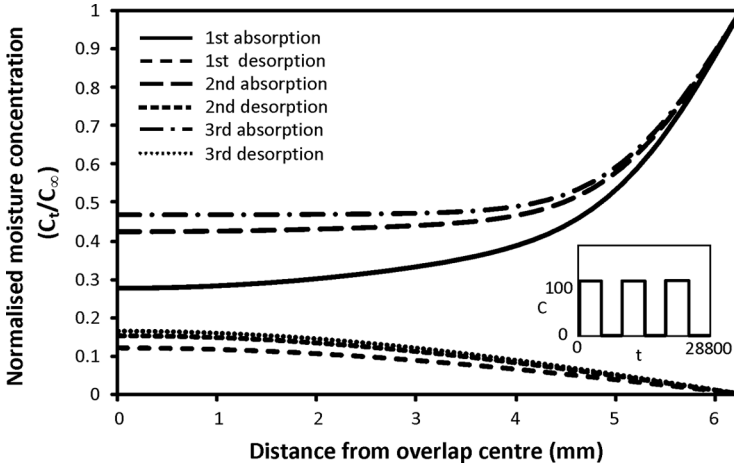


FIGURE 11 Moisture concentration in the adhesive layer after absorption-desorption cycles of 4800 h each.

the adhesive layer is reduced when the cycle time is increased to 9600 h, as shown in Fig. 12. Owing to the increased absorption time, less residual moisture is predicted in the adhesive layer during each desorption of 9600 h. As water distribution in the adhesive layer is more homogeneous than with the 4800 h cycles, the difference between

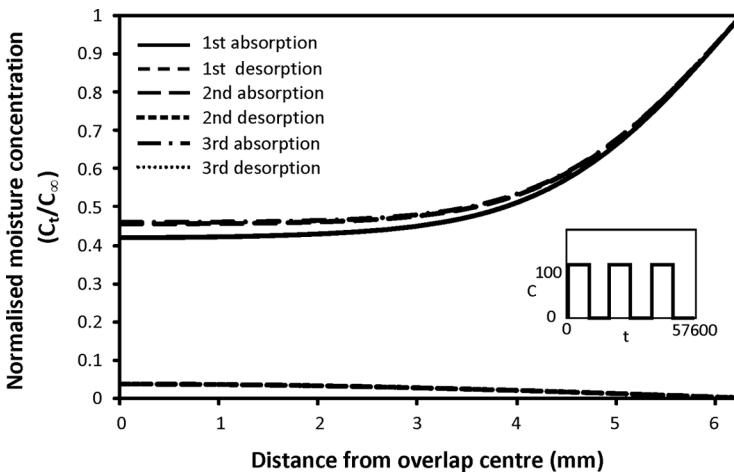


FIGURE 12 Moisture concentration in the adhesive layer after absorption-desorption cycles of 9600 h each.

residual moisture at the centre of adhesive layer after repeated cycles is greatly reduced.

5.2. Case II: Predictive Modelling Using Diffusion Parameters Based on Multiple Diffusion Cycles

To demonstrate the effects of history-dependent diffusion characteristics on moisture concentration prediction, the modelling methodology described in Section 4.2 was applied to a single lap joint subjected to the same environmental conditions as that for Case I in Section 5.1. Figure 13 compares the concentration profiles at the middle of the adhesive layer for the 4800 h cyclic conditioning environment. The predicted concentration after the first absorption processes is similar for both Case I and II, as seen by comparing Figs. 11 and 13, since the diffusion coefficients are the same for the first absorption. However, because of the faster desorption, the amount of residual moisture after the first desorption is less in Case II than in Case I. The moisture concentration after the second absorption was higher in Case II even though the amount of the residual moisture was less at the start of the absorption than in Case I. This was because of the effect of using moisture-dependent absorption coefficients. The third absorption, in Case II, also predicted a higher moisture concentration than in Case I.

In the case of 9600 h cycles, the moisture concentration in the first absorption is the same in both cases, as may be seen in Figs. 12 and 14.

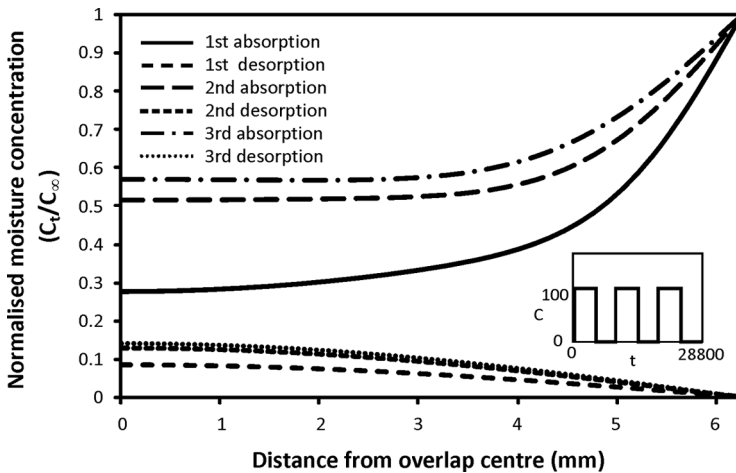


FIGURE 13 Moisture concentration in the adhesive layer, using multi-cycle model, after absorption-desorption cycles of 4800 h each.

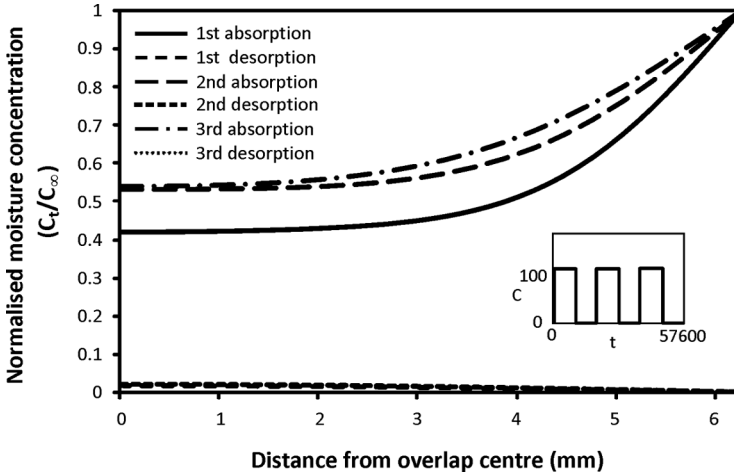


FIGURE 14 Moisture concentration in the adhesive layer, using multi-cycle model, after absorption-desorption cycles of 9600 h each.

In the second absorption, higher moisture concentration is predicted in Case II than in Case I and the moisture absorption predicted after the third absorption is also higher in Case II than in Case I, which is consistent with the predictions with the 4800 h cycles. The residual moisture after each desorption is also lower in Case II than in Case I. The longer cycles also result in lower residual moisture at the end of the desorption cycles.

6. DISCUSSION

Moisture cycling affects polymers in several ways including: the increased free volume due to swelling [16], the reaction of water with the polymer, leaching of material, micro-cracking, and the progressive damage mechanisms. Carter and Kibler [27] suggested that water in a polymer can exist in free or bound states. If there are chemical reactions between the polymer and the water, the water becomes attached to the polymer and is not free to move, whereas, the water present in the free volume of the polymer is free to move. The free volume exists in a polymer due to the gaps between the polymer chains and depends on the density and physical state of the polymer. The diffusion of water in a polymer depends on the available free volume within the polymer; a higher free volume results in a higher capacity for absorption of water. A Langmuir-type model was suggested by Carter and

Kibler to predict the moisture concentration, which has additional parameters to those used in Fickian diffusion; the probability that bound water may be released and the probability that free water may become bound. It has also been suggested that during initial moisture uptake, the moisture enters the free volume of the polymer, which does not cause swelling of the polymer [28]. During later stages, when most of the free volume is filled, the absorbed moisture distorts

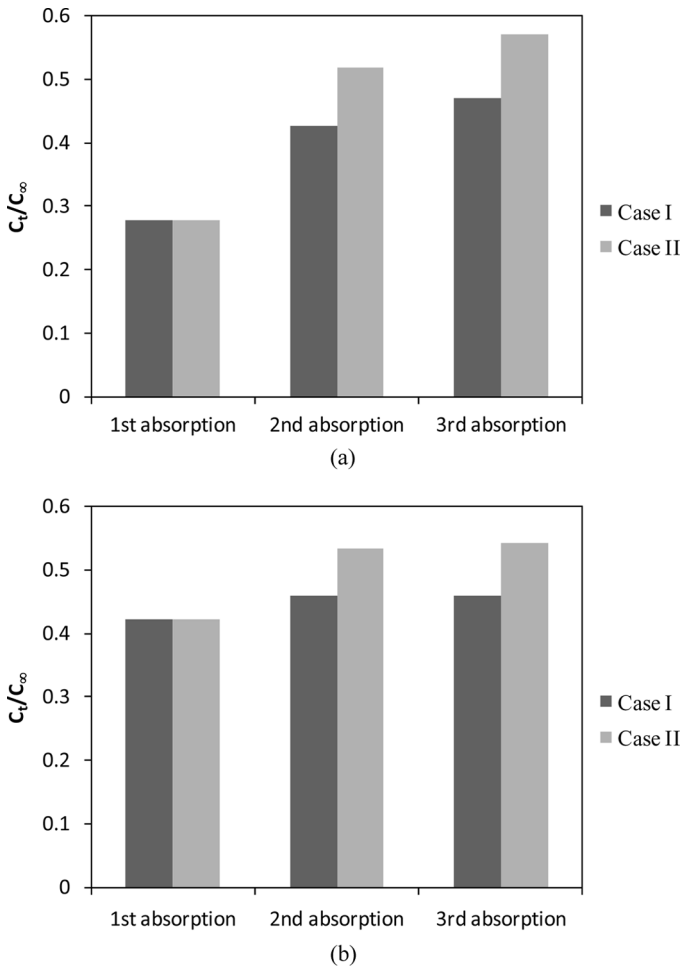


FIGURE 15 Normalised moisture concentration at the overlap centre after absorption for (a) 4800 h and (b) 9600 h conditioning.

the polymer network and causes swelling. As the polymer swells, additional free volume may become available for diffused water.

It may be seen from Fig. 3 that the absorption-desorption cycles affect D and M_∞ in a different manner. The rapid initial uptake of water by the adhesive may occur as water occupies the free volume of the adhesive. In later stages of sorption, swelling of the adhesive occurs and a lower value of D is observed. In addition to swelling, the interaction of water may also cause micro-cracking and chain

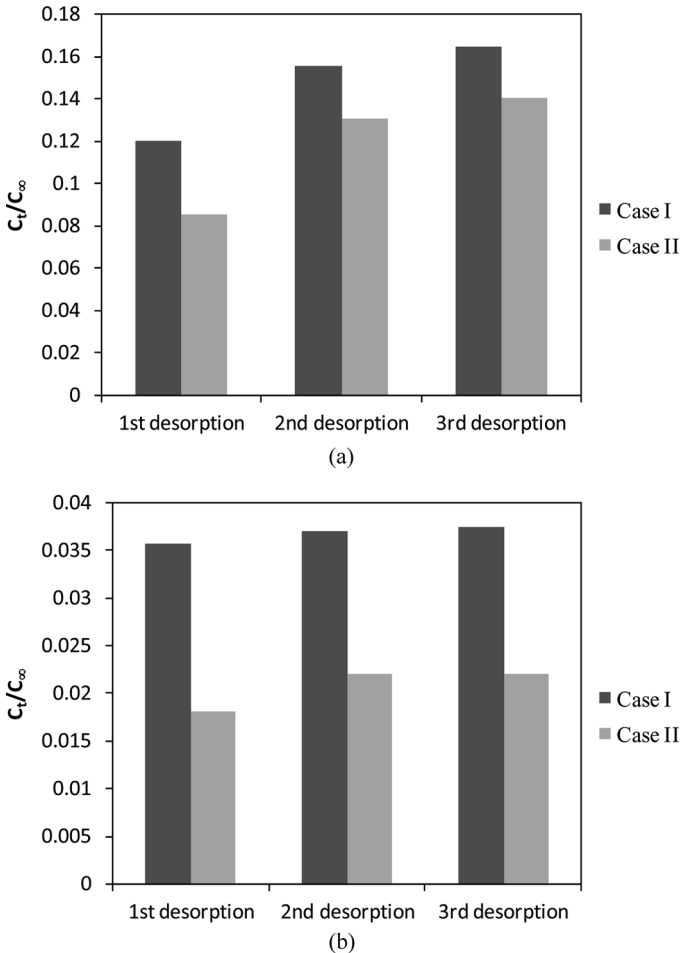


FIGURE 16 Normalised moisture concentration at the overlap centre after desorption for (a) 4800 h and (b) 9600 h conditioning.

scission of the adhesive, resulting in more sites for absorption becoming available. During the desorption, a Fickian diffusion curve indicates that free water diffusion is the predominant process as any bound water is less able to detach due to the chemical attachment. However, it is also possible that chain scission can lead to mass loss by leaching of the adhesive [29].

Comparison of the modelling methodologies where the effect of hygroscopic history is ignored (Case I) and included (Case II) show that the predicted moisture concentrations were different in both cases. This is true for absorption as well as desorption cycles. The predicted concentration after absorption in Case II either increases or stays the same between cycles and has no clear trend under different absorption times, as shown in Figs. 15(a) and (b). Thus, the amount of moisture in the adhesive layer, along with history-dependent diffusion coefficients, present a unique diffusion situation in each absorption cycle, which is difficult to predict based on a general pattern.

In general, the desorption cycles in Case II predicted a lower residual moisture at the end of each cycle than Case I, as can be seen in Figs. 16(a) and (b). This is the result of the use of moisture-dependent diffusion coefficients, which increase with each desorption cycle. The lower predicted moisture when using history-dependent moisture uptake may mean that higher strength is retained by the adhesive after desorption. The residual moisture in Case I and Case II followed the same trend as it either increased or remained the same. This is true for the 4800 h cycle as well as the 9600 h cycle.

7. CONCLUSIONS

The experimental investigation of cyclic moisture diffusion showed that the absorption of moisture in the adhesive is a non-Fickian process and the rate of absorption varies with the moisture history of the adhesive. Desorption is a Fickian process; however, the rate of desorption increases with moisture cycling. M_∞ increased because of moisture cycling. The observed change in the nature of the absorption and desorption processes with cycling indicates that the structure of the adhesive is changed by moisture absorption.

A comparison of moisture predictions based on diffusion parameters from a single absorption curve (Case I) and history-dependent diffusion parameters (Case II) revealed that the amount of residual moisture predicted in Case I is always greater than in Case II. If equilibrium is not reached during a cyclic situation, localised desorption and absorption processes occur in the adhesive layer and the use of the corresponding diffusion coefficients is necessary for a correct

moisture prediction. Neglecting the moisture history-dependent diffusion coefficient can result in over or under prediction of moisture during absorption. Since the diffusion rates in absorption and desorption are different and also have different dependencies on moisture history, it is necessary to use a methodology including moisture history for accurate prediction of degradation and residual joint strength of environmentally cycled adhesive joints.

REFERENCES

- [1] Hand, H. M., Arah, C. O., McNamara, D. K., and Mecklenburg, M. F., *Int. J. Adhesion and Adhesives* **11**, 15–23 (1991).
- [2] Liljedahl, C. D. M., Crocombe, A. D., Wahab, M. A., and Ashcroft, I. A., *The Journal of Adhesion* **82**, 1061–1089 (2006).
- [3] Minford, J. D., *Handbook of Aluminum Bonding Technology and Data*, (Marcel Dekker, Inc., New York, 1993).
- [4] Wahab, M. A., Ashcroft, I. A., Crocombe, A. D., and Shaw, S. J., *The Journal of Adhesion* **77**, 43–80 (2001).
- [5] Brewis, D. M., Comyn, J., and Tredwell, S. T., *Int. J. Adhesion and Adhesives* **7**, 30–32 (1987).
- [6] Masaro, L. and Zhu, X. X., *Prog. Polym. Sci.* **24**, 731–775 (1999).
- [7] Wilde, W. P. D. and Shopov, P. J., *Composite Structures* **27**, 243–252 (1994).
- [8] Dewimille, B. and Bunsell, A. R., *J. Phys. D: Appl. Phys.* **15**, 2079–2091 (1982).
- [9] Popineau, S., Rondeau-Mouro, C., Sulpice-Gaillet, C., and Shahnahan, M. E. R., *Polymer* **46**, 10733–10740 (2005).
- [10] Roy, S., Xu, W. X., Park, S. J., and Liechti, K. M., *J. Appl. Mech.* **67**, 391–396 (2000).
- [11] Loh, W. K., Crocombe, A. D., Wahab, M. A., and Ashcroft, I. A., *Int. J. Adhesion and Adhesives* **25**, 1–12 (2005).
- [12] Wahab, M. A., Crocombe, A. D., Beevers, A., and Ebtehaj, K., *Int. J. Adhesion and Adhesives* **22**, 61–73 (2002).
- [13] Roy, S., *J. Comp. Mater.* **33**, 1318–1342 (1999).
- [14] Lefebvre, D. R., Dillard, D. A., and Ward, T. C., *J. Adhesion* **27**, 1–18 (1989).
- [15] Lefebvre, D. R., Dillard, D. A., and Brinson, H. F., *J. Adhesion* **27**, 19–40 (1989).
- [16] Lin, Y. C. and Chen, X., *Polymer* **46**, 11994–12003 (2005).
- [17] Cytec Engineered Materials. *Datasheet-FM73 Toughened Epoxy Film*, (Cytec Industries, Inc., Woodland Park, NJ, 1998).
- [18] BS EN ISO 62:1999, *Plastics – Determination of Water Absorption*, (British Standards Institution, London, 1999).
- [19] Baker, A., Rose, F., and Jones, R., (Eds.) *Advances in the Bonded Composite Repair of Metallic Aircraft Structure*, First Ed., (Elsevier Science Ltd., London, 2002), Vol. 1.
- [20] De Neve, B. and Shanahan, M. E. R., *Int. J. Adhesion and Adhesives* **12**, 191–196 (1992).
- [21] *Mathcad 14 Help*. (Parametric Technology Corporation, Needham, MA, United States, 2007).
- [22] Liljedahl, C. D. M., Crocombe, A. D., Wahab, M. A., and Ashcroft, I. A., *Int. J. Adhesion and Adhesives* **27**, 505–518 (2007).
- [23] Hua, Y., Crocombe, A. D., Wahab, M. A., and Ashcroft, I. A., *J. Adhesion* **82**, 135–160 (2006).

- [24] Crocombe, A. D., Hua, Y., Loh, W. K., Wahab, M. A., and Ashcroft, I. A., *Int. J. Adhesion and Adhesives* **26**, 325–336 (2006).
- [25] Carslaw, H. S. and Jaeger, J. C., *Conduction of Heat in Solids*, (Oxford University Press, Oxford, 1959), 2nd Ed.
- [26] Crank, J., *The Mathematics of Diffusion*, (Clarendon Press, Oxford, 1975), 2nd Ed.
- [27] Carter, F. G. and Kibler, K. G., *J. Comp. Mater.* **12**, 118–131 (1978).
- [28] Adamson, M. J., *J. Mat. Sci.* **15**, 1736–1745 (1980).
- [29] De Neve, B. and Shanahan, M. E. R., *J. Adhesion* **49**, 165–176 (1995).